On an empirical investigation of the structural behaviour of robots

C. Doukas, J. Pandremenos, P. Stavropoulos, P. Fotinopoulos, G.Chryssolouris[1]

[1]Laboratory for Manufacturing Systems and Automation, Department of Mechanical Engineering and Aeronautics
University of Patras, Greece

Abstract
In the paper, the structural behaviour of industrial robots is investigated. The objective is the development of a model, capable of predicting the robot's accuracy, under certain arm positions and loading conditions. The Finite Element Method (FEM) is used for the model's development. An extended investigation into the total robot accuracy of the joint effect is conducted. The accuracy of the robot, under ranging loads at different positions, has been mapped and discussed.

Keywords (3 maximum):
Robot, Stiffness

1 INTRODUCTION

In order for the manufacturing industry to increase its production flexibility, it has been proposed that the milling machines be substituted with robots [1]. However, the accuracy and repeatability (+-0.07mm) of a typical robotic arm [2] is not as high as this of an ordinary CNC milling machine with typical value of ±0.016 mm or better [3]. Since the accuracy issues affect the quality of the final product, they have to be resolved in order for the penetration of machining robots to be increased in industry.

This paper focuses on the modeling of a robotic arm, in FE environment. The purpose is to simulate its behavior under various loading scenarios and create a visual representation of the robot's performance in its working envelop, in terms of accuracy.

Developments in machining and tool design technology, especially in milling operations, reflect the requirements for flexibility in order to adapt the changes taking place in the market and in the global economic environment [1]. Makhanov et al. [4] presented a new approach to tool-path optimization of milling robots, based on a global interpolation of the required surface by a virtual surface composed of tool trajectories. Kao et al. [5] presented a robot-based computer-integrated manufacturing (CIM) automation. Abele et al. [6] described the modeling of the robot structure and the identification of its parameters focusing on the analysis of the system's stiffness and its behavior during the milling process.

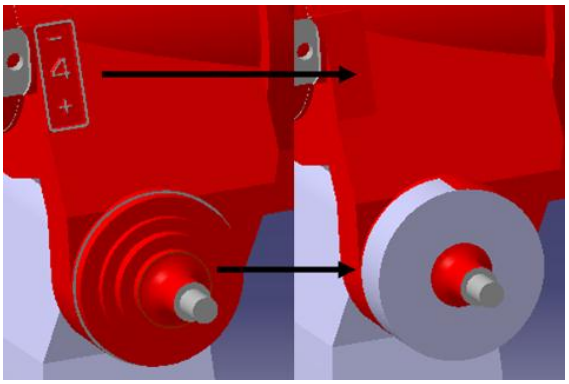

Figure 1 : Illustration of simplifications (right) performed on the robot model

2 MODELLING APPROACH

2.1 GEOMETRY

The study was conducted using a six degrees of freedom robot of 130kg payload [2]. The CAD files were imported as STP file in a CAD environment in order for the geometric model of the robotic arm to be created and then exported to the FE environment.

A number of geometrical simplification/modifications were required in order for the model to be correctly imported into the FE environment. These changes affect the meshing quality of the geometry as well as the computational time requirements. All changes were kept to the absolutely minimum, in order to allow correct meshing, but without affecting the accuracy of the results (Fig. 1).

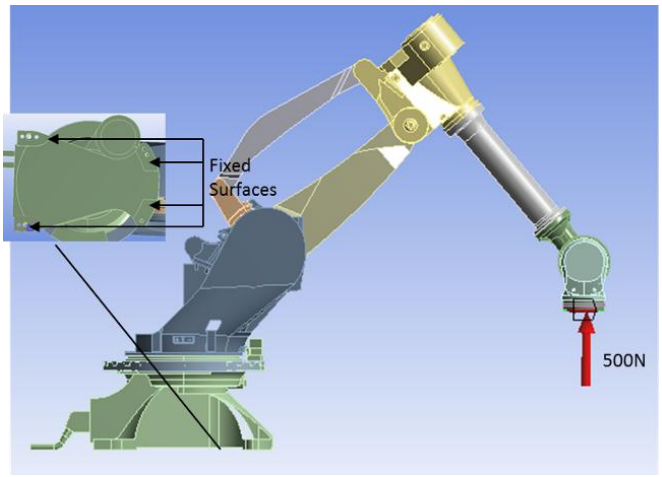

Figure 2: Force application vector and applied constraints

2.2 FE SIMULATION

The geometric model was imported as a static case into FE environment in order to simulate the effect of the loads applied to the flange end-effector during a milling process.

All the parts are considered being deformable bodies and the material used is structural steel. The properties data set used is shown in Table 1 [7].

Property	Value
Tensile Yield Strength	250 Mpa
Compressive Yield Strength	250 MPa
Tensile Ultimate Strength	460 Mpa
Young Modulus	200GPa
Poison ratio	3,00E-01
Density	7850 kgm^{-3}
Coefficient of thermal expansion	0,000012 c^{-1}
Ductility coefficient	0,213
Ductility Exponent	-0,106
Strength Coefficient	920 Mpa
Strength Exponent	-0,106
Cyclic Strength Coefficient	1 Gpa
Cyclic Strain Hardening Exponent	0,2

Table 1: Mechanical properties of the applied material

The loading scenario used in the given simulation is presented in Fig.2. The base of the arm is fixed and the appropriate load is applied to the robot end-effector.

All constraints between the assembly parts were added manually to the axes of rotation with the use of the tool of the FE environment provided.

For the original model, part connectivity was assigned to be Fixed or Revolute, which later allows the user to manipulate the static position of the arm so as for the simulation to be performed in different orientations.

Equivalent Stress (Von-Mises) and Total Deformation solutions were used for assessing the validity of the solutions with the default mesh element size. Deformation was selected as the target solution, while stress was added as a control to test the consistency of the solutions. These tests were run with the same loading condition in the initial robot Calibration Position and the modified orientation, Position 2 (Fig. 4b).

The results of the FE simulation are shown respectively below visually depicting the areas of increased stress and deformation by a colour scale. The maximum and minimum stresses and deformations have also been tagged (Fig. 3a, Fig. 3b).

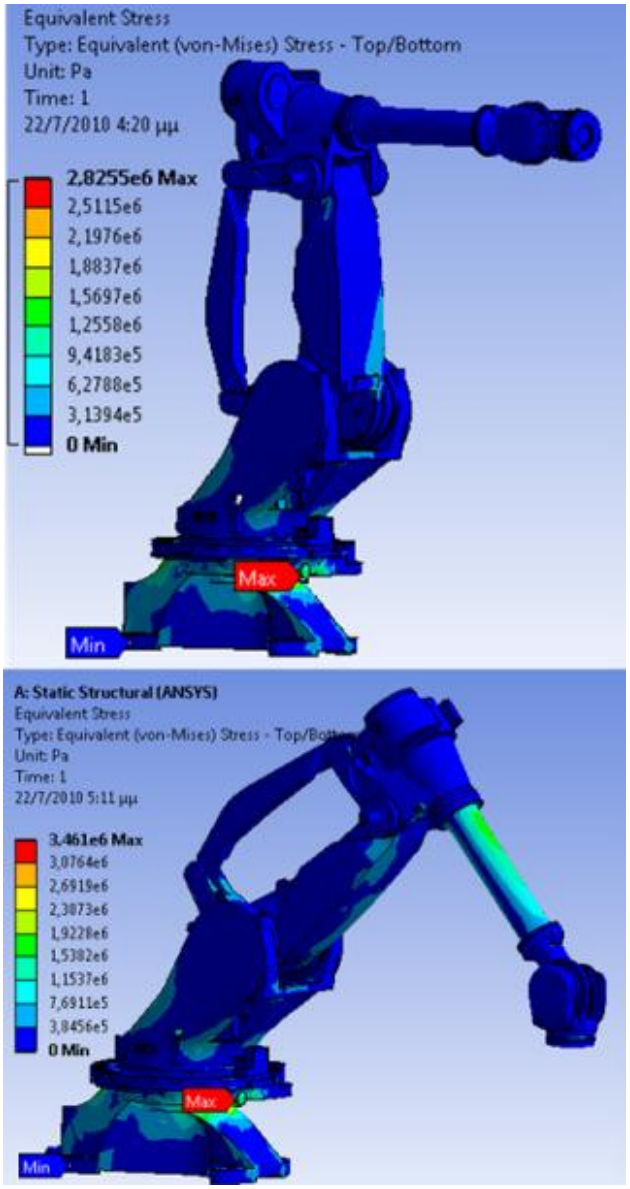

Figure 3a : Contours of Equivalent Stress (applied force of 500N, supported at base

The final element size selected was 0.03m.

In order for the model to further be developed and higher accuracy level to be achieved, three models with different configurations have been tested. The initial model *(Model 1)* was used as the base for the other two (improved) versions. The difference of each model lies in the connection type of the mating parts.

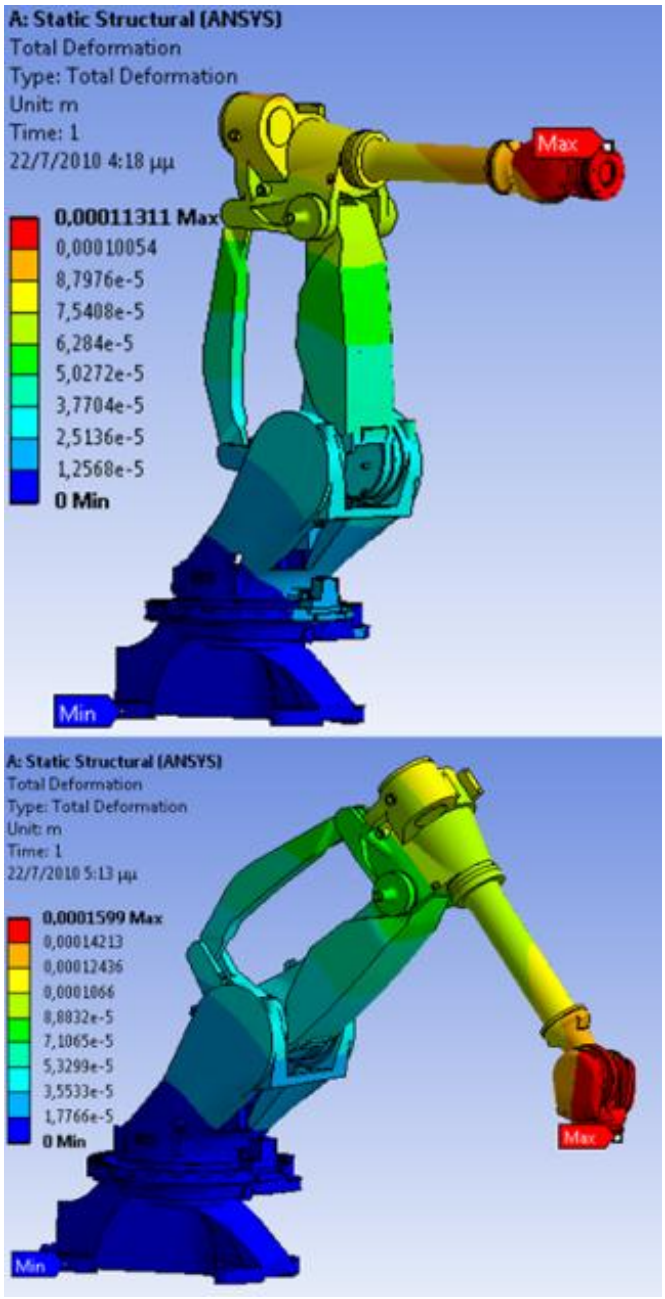

Figure 3b : Contours of Total Deformation (applied force of 500N, supported at base

2.3 **Model 1**

For the first model, the connections among the different parts of the robot assembly structure are defined as fixed to each other, so as to simulate only the elastic behavior of the arm itself. This means that the boundary faces of each part's joints of the robot structure cannot move in regard to the adjacent parts. The ''standard mechanical'' option set has been used with the ''Normal Stiffness'' option.

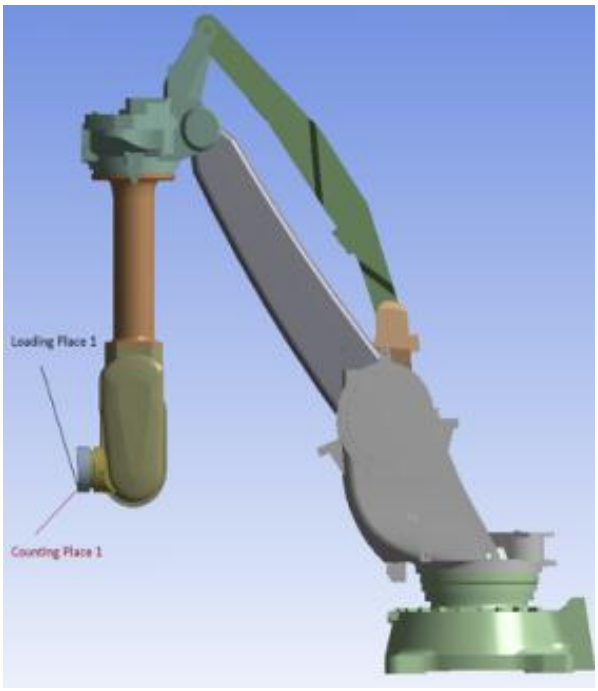

Figure 4a: Simulation position 1

2.4 **Model 2**

Model 2 is identical to Model 1, concerning the connections type between the body parts except for the changes to contacting surfaces selection and adjustments of the model behaviour and the formulation method [8].

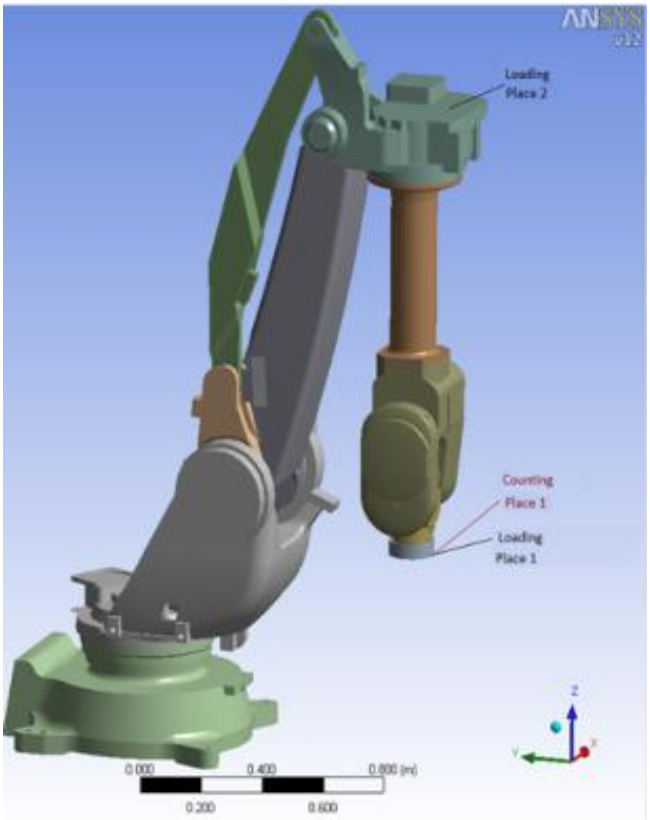

Figure 4b: Simulation position 2

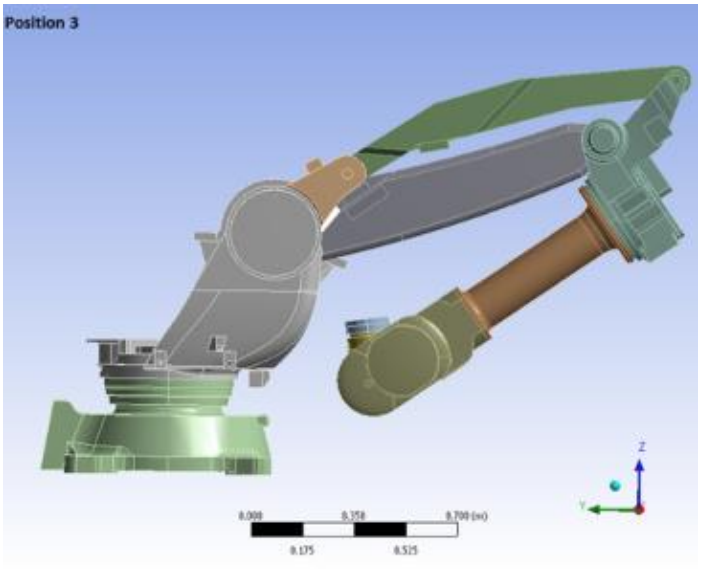

Figure 3: Simulation pose 3 (Side view).

2.5 **Model 3**

The precision of model 3, has greatly improved after the limited stiffness of the robot joints having been taken into consideration by simulating them with a calculated torsional stiffness value (Table 3). The ‘‘standard mechanical’’ option set has been used with the manual stiffness options (Auto asymmetric behavior and augmented Lagrange method).

Model 3	Type of Contact
Part 1 to Part 3	No Separation
Part 2 to Part 6	Bonded
Part 3 to Part 5	No Separation
Part 4 to Part 6	No Separation
Part 4 to Part 8	No Separation
Part 5 to Part 10	No Separation
Part 5 to Part 7	No Separation
Part 7 to Part 10	No Separation
Part 1 to Part 10	No Separation
Part 2 to Part 3	No Separation
Part 7 to Part 9	No Separation
Part 5 to Part 10	No Separation
Part 7 to Part 9	No Separation
Part 7 to Part 10	No Separation

Table 2: Type of contact used

3 RESULTS

A number of validation and data gathering experiments have been conducted.

From the experimental data, it is obvious that the main effect on the end-effector deformation is the torsional stiffness of the joints and especially, the robot’s first three axes.

The main adaptation performed to the FE model is the calculation of the torsional stiffness of all joints by running multiple simulations and adapting the torsional stiffness values in order to approximate the experimental values of deformation.

Connection type	Torsional Stiffness (kNm/$^{o)}$
Part 8 to 4	20
Part 4 to 6	20
Part 2 to 3	23
Part 3 to 5	13
Part 3 to 1	0
Part 1 to 10	0
Part 5 to 10	13
Part 5 to 7	43
Part 7 to 9	28

Table 3: Joint stiffness implemented value

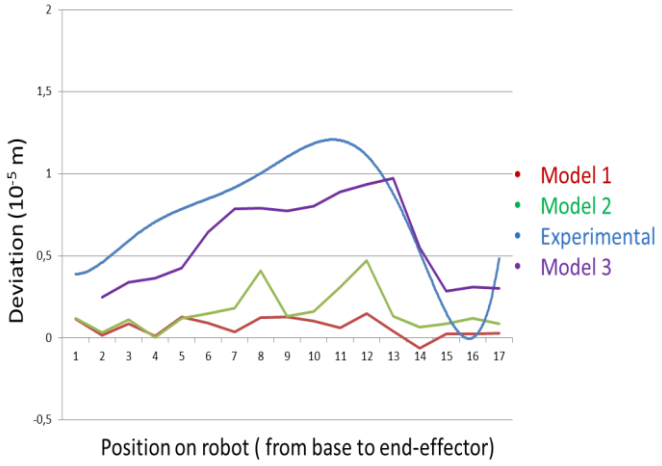

Figure 4: Comparison of experimental data to FE results

For the verification of the original assumption that the main contributors to the end-effectors deflexion are the robot joints and that the actual stiffness of the body is not a critical aspect in our case, multiple measurements have taken place for the same robot position and load case. Especially, for the exclusion of the “unaffected” axes effect, loads were applied to selected positions of the robot body, after specific joints whose effect on the robot behaviour were under investigation, while the deflexion was measured at the same position, instead of the robot’s end-effector. This way, only the effect of the joints before the load-point was taken into consideration and clear data can be gathered to be entered into the FE model.

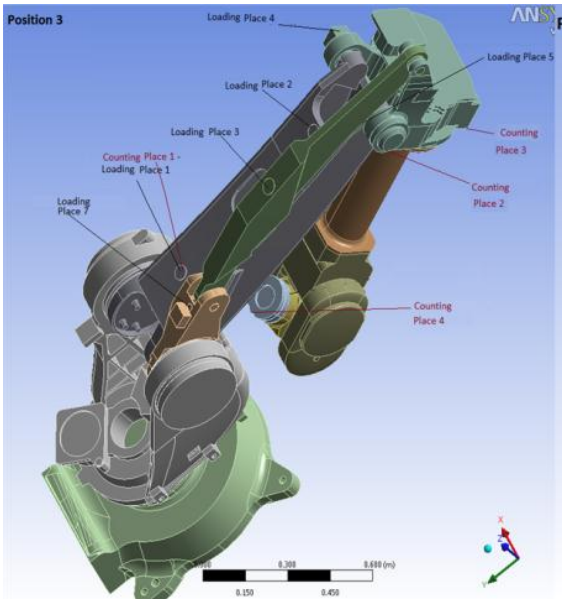

Figure 5 : Model in position No.3 – Load and measuring points are displayed

4 DEFLECTION MAP

To visually demonstrate the magnitude of the robot's end effect deflection under loading conditions, a map was created visualizing the results of FE simulations, in various spots of the workspace. Each point is color coded so as to clearly depict the deflection range. The result that is a color graded diagram and shows the sum of deflection in every position of each simulation was categorized according to the deviation value into 5 classes.

The load case used consists of 500N horizontally and 500N vertically in a direction that opposes the movement of the end effector [9].

Horizontal (Fig. 9) and vertical (Fig. 10) maps have been plotted in separate diagrams, so as to independently show the deflection of the end effector in the working envelop of the robot.

In that way, it is possible for one to see at a glance, the positions that should be avoided and those that are the most preferable in order for the loss of accuracy to be minimized in a high load robotic operation.

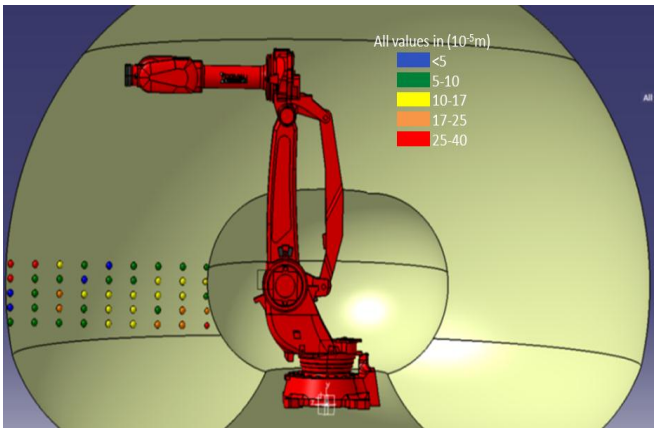

Figure 6 : Horizontal Deflection Map

5 DISCUSSION

Industrial Robots can considerably contribute to improving the flexibility of machining operations. Their high level of flexibility and extended working space can outperform the conventional machine tools. Due to their extra degree of freedom, an industrial robot can machine complicate geometries that otherwise would need special fixturing elements and multiple machining operations.

On the other hand, it is clear that robots possess serious disadvantages in terms of accuracy, repeatability and handling in machining processes, when they are being compared with the conventional CNC machine tools. This is due to their low absolute positioning accuracy and repeatability.

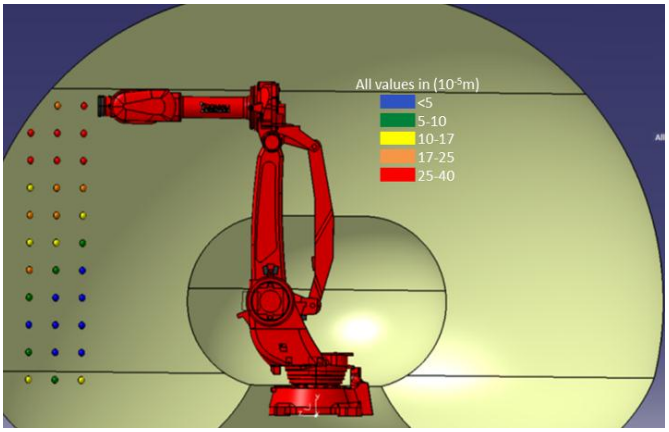

Figure 7 : Vertical Deflection Map

The creation and implementation of an FE based model can accurately simulate the behavior of a typical industrial robot, as long as the necessary requirements (accurate CAD designs, material properties and loading conditions) are available. By using the FE modeling results and comparing them with the experimental data available, the model can be fine-tuned to further improve the accuracy of simulation.

Moreover, the construction of the deformation map of the robot's workspace, the area with the highest accuracy results, can be selected for any given machining scenario, thus, improving the accuracy of the machining process even further.

6 CONCLUSIONS

The accuracy of the original model in comparison with that of the experimental data has shown extended deviations. In order for these deviations to be confronted in the new model created, the changes were incorporated into the joint properties to approach the actual robot behavior. The model was counterpoised with experimental data and through adjustments of the joint stiffness value, the model was fine tuned. Further experiments, on the actual robot arm, showed that the model followed the actual behavior of the robotic arm, with minimum deviations.

To better depict the model accuracy, a deflection map has been created, clearly showing the simulated accuracy of the model in the workspace of the robot arm.

7 ACKNOWLEDGMENTS

The research leading to these results has received funding from the European Union's seventh framework program (FP7/2007-2013) under grant agreements #258769 (COMET: Plug-and produce **CO**mponents and **MET**hods for adaptive control of industrial robots enabling cost effective, high precision manufacturing in factories of the future).

8 REFERENCES

[1] Chryssolouris, G. 2006. *Manufacturing systems – theory and practice 2nd ed.* New York : Springer-Verlag, 2006

[2] Comau. 2008. Comau Robotics Downloads. *Comau.* [Online] http://www.comau.com/DlDownload/Smart5%20NJ%2010-3.0%20CAD%20(3D-STEP)/SMART-5%20NJ-110-3.0%20(3D-STEP).zip.

[3] HassAutomation. 2011 Hass Automation, Inc. *VR-8 SPECIFICATIONS.* http://www.haascnc.com/lang/specs.asp?ID=VR-8&intLanguageCode=1033&webid=VMC_5AXISSPINDLE#VMCTreeModel.

[4] Makhanov, S.S., et al. 2002. On the tool-path optimization of a milling robot. *Computer & Industrial Engineering.* 2002, Vol. 43, 3, pp455-472, pp. 455-472.

[5] Kao, I. and Gong, C. 1997. Robot-based computer-integrated manufacturing as applied in manufacturing automation. *Robotics and Computer - Intergrated Manufacturing.* 1997, Vol. 13, 2, pp157-167, pp. 157-167.

[6] Abele, E., Weigold, M. and Rothenbücher, S. 2007. Modeling and Identification of an Industrial Robot for Machining Applications. *CIRP Annals - Manufacturing Technology.* 2007, Vol. 56, 1, pp387-390, pp. 387-390.

[7] Comau. 2008. Smart5 NJ 110-130 Technical Specifications. *Comau.* [Online] 2008. [http://www.comau.com/DlDownload/Smart5%20NJ%2011030%20Technical%20Specifications/Smart%205%20NJ

[8] ANSYSWorkbench. Release 11.0 Documentation for ANSYS Workbench. *Formulation Metods.* [Online] [Cited: Dec 15, 2011.] http://www.kxcad.net/ansys/ANSYS/workbench.

[9] Carr Lane Manufacturing Co. Carr Lane USA Catalog. *Carr Lane USA.* [Online] [Cited: Dec 19, 2011.] http://www.carrlane.com/Catalog/index.cfm/29625071F0B221118070C1C513906103E0B05543B0B012009083C3B28535140594820131 80B041D1E173C3B2853524B5A59.